DOI 10.1007/s11182-015-0373-4

*Russian Physics Journal, Vol. 57, No. 9, January, 2015 (Russian Original No. 9, September, 2014)*

# INTERMARTENSITIC THERMOELASTIC TRANSFORMATIONS IN [012]-ORIENTED SINGLE CRYSTALS OF FERROMAGNETIC NIFEGA ALLOYS UNDER COMPRESSIVE LOADING

**E. E. Timofeeva, E. Yu. Panchenko, Yu. I. Chumlyakov, and A. I. Tagiltsev**

UDC 669.24'1'871-539.371:548.55

*The results of investigations of stress-induced intermartensitic transformations in [012]-oriented* $Ni_{54}Fe_{19}Ga_{27}$ *(at.%) single crystals are presented as a function of testing temperature and applied stresses. The sequence of intermartensitic transformations* $L2_1$*–14M–*$L1_0$ *at* $T < 423$ *K is observed to change to* $L2_1$*–*$L1_0$ *at* $T > 423$ *K. The interval of superelasticity development is controlled by the high value of* $\alpha_{2-1} = d\sigma_{cr}/dT = 3.1$ *MPa/K and on the side of high temperatures is limited by the strength properties of the martensite phase; superelasticity is observed during* $L2_1$*–14M–*$L1_0$*-transformations below 353 K. It is experimentally found out that with increasing temperature and externally applied stresses the value of reversible transformation-induced strain is decreased, while the stress hysteresis is increased, and the interval of the forward transformation under loading becomes larger than that of the reverse.*

**Keywords:** thermoelastic intermartensitic transformations, superelasticity, reversible deformation, yield strength level of the martensite.

## INTRODUCTION

It is well known that advanced ferromagnetic NiFeGa alloys undergo martensitic transformations (MTs) under variations in temperature and application of stress and magnetic fields [1]. Note that under applied stress multistage intermartensitic transformations can develop [2, 3]: the cubic $B2(L2_1)$-lattice of the austenite can either immediately transform to form tetragonal $L1_0$-martensite or through the intermediate layered, long-period, modulated structures 10*M* and 14*M*. Every type of strain-induced martensite (10*M*, 14*M*, $L1_0$) is characterized by different values of lattice strain and critical stresses causing formation and motion of twin boundaries in the martensite, which is exhibited as a series of stages in the $\sigma(\varepsilon)$, $\varepsilon(T)$ and $\sigma_{cr}(T)$ curves under conditions of the shape memory effect (SME) and superelasticity (SE) [2, 3]. Thus, being able to control the sequence of intermartensitic transformations is critical for designing alloys with a set of predetermined functional properties, including propensity for magnetically-induced deformations. Therefore, in order to control the functional properties of shape-memory NiFeGa ferromagnetic alloys and their future practical applications, we need systematic investigations of the mechanisms and behavior of martensitic transformations in them. Polycrystalline NiFeGa alloys fail along grain boundaries in the course of evolution of MTs due to the high values of crystal anisotropy $A = 2C_{44}/(C_{11} - C_{12}) > 10$, which makes their investigation and application difficult [4]. Using NiFeGa single crystals, it was found out [2, 3, 5–7] that the sequence of intermartensitic transformations is controlled by the orientation of crystals and stress state: martensitic transformations were investigated in NiFeGa single crystals oriented along [001]-, [011]- and [012]-directions [2, 3, 5–7]. The deformation induced by transformation is shown to

The National Research Tomsk State University, Tomsk, Russia, e-mail: katie@sibmail.com. Translated from Izvestiya Vysshikh Uchebnykh Zavedenii, Fizika, No. 9, pp. 105–113, September, 2014. Original article submitted April 9, 2014.

 

TABLE 1. Theoretically Calculated Transformation Strains $\varepsilon_{CVP}$ and $\varepsilon_{CVP+detw}$ in [012]-Oriented Single Crystals of Ni–Fe–Ga in Compression [2, 3]

| Martensite structure | $\lvert\varepsilon_{CVP}\rvert$,% [2, 3] | $\lvert\varepsilon_{CVP+detw}\rvert$,% [2, 3] |
|---|---|---|
| 14*M* | 4.0 | 4.1 |
| $L1_0$ | 3.95 | 6.25 |

be related to the formation of twinned martensite (CVP-structure) $\varepsilon_{CVP}$ and its subsequent detwinning $\varepsilon_{detw}$: $\varepsilon_{CVP} + \varepsilon_{detw} = \varepsilon_{CVP+detw}$. The value of $\varepsilon_{CVP+detw}$ corresponds to lattice strain $\varepsilon_0$ during transformation of a single crystal of the austenite into a single crystal of the martensite. In [001]-oriented single crystals in compression and in [011]-oriented single crystals in tension, in which the transformation strains $\varepsilon_{CVP+detw}$ during the formation of 14*M*- and $L1_0$-martensites are equal, $\varepsilon^{L1_0}_{CVP+detw} = \varepsilon^{14M}_{CVP+detw}$, and detwinning of the $L1_0$-martensite $\varepsilon_{detw}$ makes no contribution into the transformation strain $\varepsilon^{L1_0}_{CVP+detw} = \varepsilon^{L1_0}_{CVP}$, only one stage is observed in the $\sigma(\varepsilon)$ and $\sigma_{cr}(T)$ responses, which is related to a stress-induced MT. In [001]- and [012]-oriented single crystals in tension and in [011]-oriented single crystals in compression, for which $\varepsilon^{L1_0}_{CVP+detw} \neq \varepsilon^{14M}_{CVP+detw}$ and detwinning of the $L1_0$-martensite $\varepsilon_{detw}$ makes a considerable (up to 60% of the cumulative value) contribution into the deformation strain $\varepsilon^{L1_0}_{CVP+detw} \neq \varepsilon^{L1_0}_{CVP}$, the $\sigma(\varepsilon)$ and $\sigma_{cr}(T)$ responses contain a number of stages attributed to a gradual development of the $L2_1$–14*M*–$L1_0$ MTs. A change of the MT sequence from $L2_1$–14*M*–$L1_0$ to $L2_1$–$L1_0$ in the [001]- and [012]-orientations under tensile loading favors the formation of high-temperature SE up to 700 K [2, 3, 5–7]. Single crystals, oriented along the [012]-direction, have not been so far investigated in compression. In this connection, the purpose of this work is to investigate the mechanisms of development of martensitic transformations in [012]-oriented single crystals of $Ni_{54}Fe_{19}Ga_{27}$ (at.%) in the course of compressive deformation, for which $\varepsilon^{L1_0}_{CVP+detw} \neq \varepsilon^{14M}_{CVP+detw}$ and $\varepsilon^{L1_0}_{CVP+detw} \neq \varepsilon^{L1_0}_{CVP}$ (contribution from detwinning of the $L1_0$-martensite into the transformation strain $\varepsilon^{L1_0}_{detw} \sim 30\%$) (Table 1).

## 1. EXPERIMENTAL PROCEDURE

Single crystals of $Ni_{54}Fe_{19}Ga_{27}$ (at.%) were grown using the Bridgemann method in the inert-gas atmosphere. The specimens oriented along the [012]-direction for compressive tests were shaped as parallelepipeds measuring $3 \times 3 \times 6$ mm$^3$. In this study, we deal with crystals subjected to no additional heat treatment since as-grown single crystals are found in a single-phase state, and their high-temperature phase has an $L2_1$-structure [6, 7]. The development of a stress-induced MT was investigated using the $\sigma(\varepsilon)$ response during isothermal loading/unloading cycles within the temperature interval from 100 to 900 K and the $\varepsilon(T)$ response during cooling/heating under a constant load within the range of stresses from 0 to 270 MPa. The isothermal loading/unloading cycling was performed in an Instron 5969 machine and in a vacuum setup at the temperatures $T > 623$ K. The heating/cooling tests with application of external stresses were carried out in an ad hoc installation measuring reversible strain.

The starting and finishing temperatures of the forward MT ($M_s$, $M_f$) and those of the reverse MT ($A_s$, $A_f$) were derived from the electrical resistance as a function of temperature. The microstructure of single crystals was examined in a Philips CM 12 transmission electron microscope at an accelerating voltage of 120 kV. The specimen orientation was determined in a Dron-3 diffractometer using Fe$K_\alpha$-emission.

## 2. EXPERIMENTAL RESULTS AND DISCUSSION

As-grown single crystals in a high-temperature phase have an $L2_1$-structure and are found in a single-phase state [6–9], while when cooled/heated in free state, they undergo single-stage $L2_1$–14*M* MTs [6–9]. The temperatures of

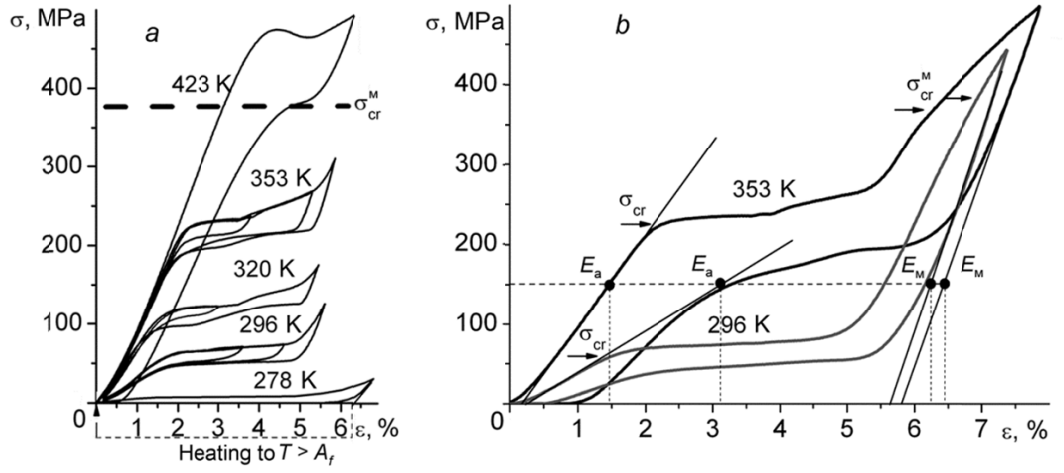


Fig. 1. Stress-strain responses σ(ε) for the [012]-oriented NiFeGa single crystals in compression: development of SE response within 278–423 K without deformation of the martensite (*a*), SE response at 296 and 353 K with deformation of the martensite (*b*).

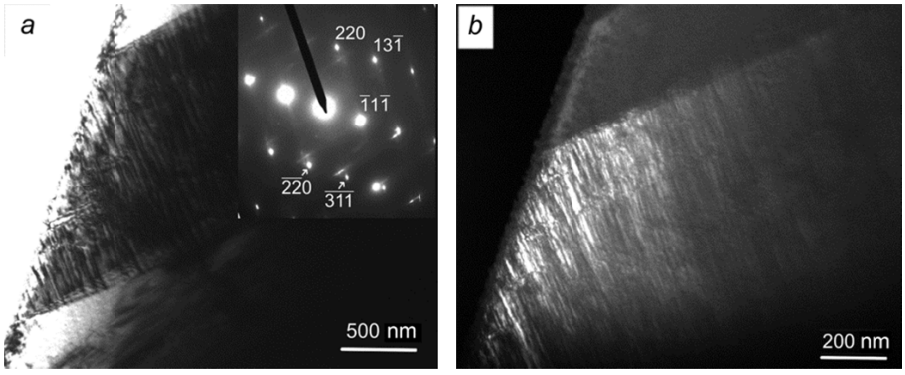


Fig. 2. Microstructure of the [012]-oriented NiFeGa single crystals after compressive deformation: at $T = 296$ K, $\varepsilon_{irr} = 1.5\%$, zone axis $[1\,\bar{1}\,\bar{2}]_{L10}$ – a bright-field image and the selected diffraction pattern (*a*) and a dark-field image in the $\bar{3}\,\bar{1}\,\bar{1}_{L10}$ reflection (*b*).

the start and finish of a forward MT are $M_s = 274$ K and $M_f = 270$ K, and those of a reverse MT are $A_s = 278$ K and $A_f = 283$ K. Figure 1 presents the σ(ε) response for [012]-oriented single crystals of NiFeGa in compression.

An analysis of the σ(ε) curves demonstrates that as the testing temperature increases, the critical stresses of the stress-induced MT, $\sigma_{cr}$, the stress hysteresis, Δσ, and the strain hardening coefficient values, $\theta = d\sigma/d\varepsilon$, are increased, while the reversible strain is decreased. Note that the yield strength level of the martensite hardly depends on temperature and is found to be 368–382 MPa (Fig. 1*b*).

During the evolution of SME and SE up to the temperature ~ 300 K, there is one stage in the σ(ε) response (Fig. 1*a*). Since the thermal-induced martensite has a 14*M*-structure, it is expected that under loading single-stage $L2_1$–14*M* MTs will also be observed. On the other hand, the maximum experimental reversible strains during SME $\varepsilon_{SME} = 6.3$ (±0.3)% exceed the theoretical value $|\varepsilon_{CVP+detw}| = 4.1\%$ for $L2_1$–14*M* and coincide with the value $|\varepsilon_{CVP+detw}| = 6.3\%$ for the case of formation of a completely detwinned $L1_0$-martensite (Table 1). TEM images of the material after deformation at $T \sim 300$ K reveal residual $L1_0$-martensite (Fig. 2). This suggests that during SME and SE developing up to $T \sim 300$ K, there is an $L2_1$–14*M*–$L1_0$-sequence of MTs.

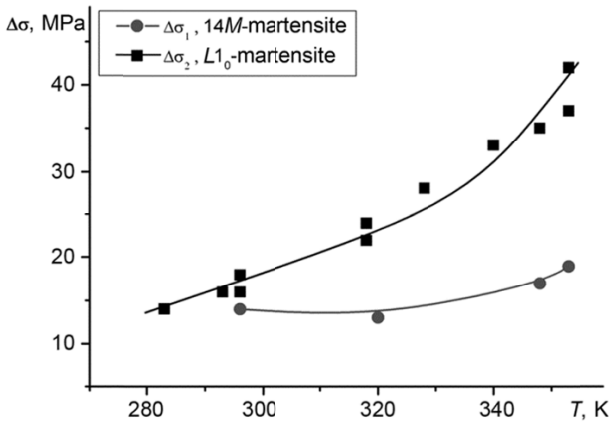


Fig. 3. Dependence of the stress hysteresis on temperature $\Delta\sigma(T)$ for the [012]-oriented NiFeGa single crystals in compression.

No stepwise pattern associated with the development of an $L2_1$–$14M$–$L1_0$ sequence of MTs is observed in the σ(ε) response during examination of SME and SE ($T < 300$ K), because the stresses of formation of the $14M$- and $L1_0$-martensites could be the same. At the testing temperatures from 300 to 350 K, the σ(ε) curves for the [012]-oriented single crystals contain stages differing in the level of stresses and having bends (Fig. 1*a*). Under conditions of isothermal loading/unloading cycling, it is evident that at $T > 300$ K for a given strain corresponding to the first transformation stage the stress hysteresis value is small, it hardly depends on temperature, and is found to be $\Delta\sigma_1 \sim 16$ MPa (Fig. 3). The hysteresis in the second stage $\Delta\sigma_2$ is equal to $\Delta\sigma_1 \sim 17$ MPa at 296 K, but the values of $\Delta\sigma_2$ increase with temperature up to 40 MPa at 353 K (Fig. 3).

It is known from [10], that during development of an $L2_1$–$14M$ MT, the hysteresis is smaller than it is during an $L2_1$– $L1_0$ MT. First, the $14M$-martensite has a high density of twins and the lattice misfit between $14M$- and $L2_1$ structures is small, which ensures a low friction force during phase-boundary motion [10]. Second, the $14M$-martensite does not detwin under loading in contrast to the $L1_0$-martensite [10]. Therefore, the first stage corresponds to the $L2_1$–$14M$ MT, and the second – to the subsequent $14M$–$L1_0$ MT.

An increase in the hysteresis value $\Delta\sigma_2$ (corresponding to the formation of an $L1_0$-martensite) with increasing $T$ was also observed in other alloys with thermoelastic MTs [11, 12]. This could be accounted for by the Roytburd model [13], which predicts that if $\varepsilon_{CVP} \neq \varepsilon_{CVP+detw}$, then under the action of external stresses the habitus plane would trade off the invariant plane due to twinning of $L1_0$-martensite, which would give rise to additional internal stresses, whose dissipation would result in an increased hysteresis.

It is worth mentioning that above 300 K for a given strain corresponding to the development of a two-stage $L2_1$–$14M$–$L1_0$ MT, the value of hysteresis $\Delta\sigma_1$ within the first stage becomes equal to $\Delta\sigma_2$. It is assumed that the dependence of the $\Delta\sigma_1$ values on a given strain could be accounted for as follows. When a forward $L2_1$–$14M$ MT occurs under loading, in the case of unloading there is a reverse $14M$–$L2_1$ MT. Given a complete $L2_1$–$14M$–$L1_0$-transformation, the reverse MT is characterized by higher energy dissipation, and during unloading the transition from the $L1_0$-martensite into the $L2_1$-austenite occurs directly rather than via a $14M$-structure, i.e., a reverse $L1_0$–$L2_1$ MT develops.

It is critical to note that the reversible strain in the first stage is smaller than that theoretically predicted for the $L2_1$–$14M$ MT (see Table 1). A similar behavior was reported by the authors of [10], where they demonstrated that at high temperatures intermartensitic transformations $L2_1$–$14M$–$L1_0$ do not develop sequentially (formation of 100% $14M$-matensite followed by formation of 100% $L1_0$-martensite), but simultaneously, which in the σ(ε) response is observed as a single stage with a Luders – Chernov band. Accomodation of the $L2_1$- and $L1_0$-structures occurs via the region with a $14M$-structure containing higher microtwin density. During the development of an MT the volume fraction of the $14M$-martensite remains constant (~40%), while that of the $L1_0$-martensite increases. The final phase has an $L1_0$-structure [10].

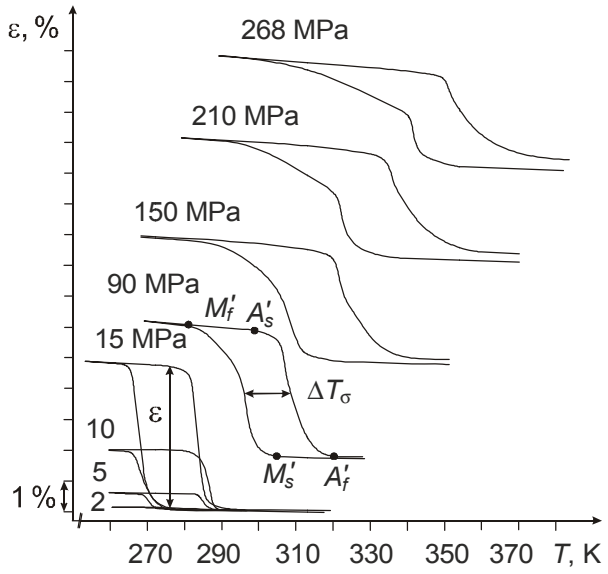


Fig. 4

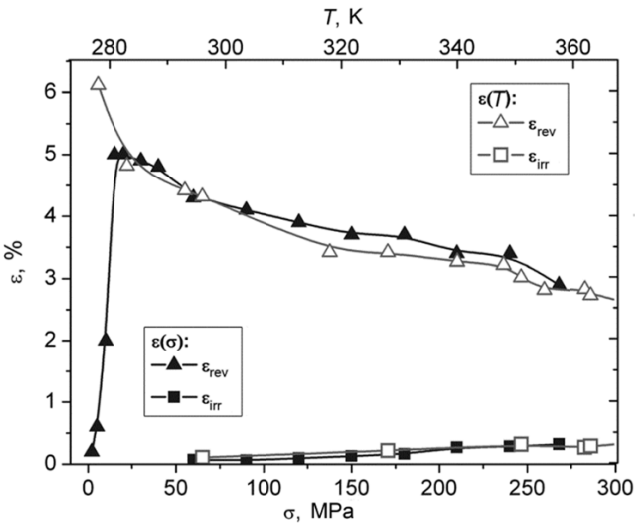


Fig. 5

Fig. 4. Strain-temperature ε(*T*) response for the [012]-oriented NiFeGa single crystals in compression.

Fig. 5. Dependences of the reversible $\varepsilon_{rev}$ and irreversible $\varepsilon_{irr}$ strain on the testing temperature *T* and external stresses σ, which were obtained from the σ(ε) and ε(*T*) responses for the [012]-oriented NiFeGa single crystals.

The formation of stages in the σ(ε) curves at $T > 300$ K and an increase in the values of strain hardening coefficient and stress hysteresis are related to a more difficult process of detwinning of the $L1_0$-martensite at elevated temperatures and could be due to the low yield strength level of the martensite (see Fig. 1).

Figure 4 presents the ε(*T*) response for the [012]-oriented single crystals of NiFeGa during cooling/heating under constant compressive loading. In free state during cooling a self-accommodating system is formed in the specimen and it does not change its dimensions. Similarly, at the minimum applied stresses 2 MPa, the volume fraction of the oriented martensite approaches zero $\delta^M \rightarrow 0$. With increasing external applied stresses $\sigma > 2$ MPa $\delta^M$ increases, and at $\sigma = 15$ MPa the reversible strain attains its maximum value 5% (Fig. 4). Thus, the [012]-oriented single crystals are characterized by low resistance to phase- and twin-boundary motion.

The ε(*T*) and σ(ε) responses are consistent with each other, which is also demonstrated by the curves of the reversible strain $\varepsilon_{rev}(T)$ and $\varepsilon_{rev}(\sigma)$, represented in Fig. 5, and the $\sigma_{cr}(T)$ and $M_s'(\sigma)$, represented in Fig. 6*a*. For instance, at the temperature $T = 283$ K, the stresses needed for an MT to start are $\sigma_{cr} = 30$ MPa. For the case where the applied external stress is 30 MPa, under cooling an MT begins at $M_s' = 283$ K. The reversible strain values in these points coincide and are equal to 4.8%.

We have experimentally found out that with increasing testing temperature and compressive stresses the reversible strain $\varepsilon_{rev}$ decreases (Figs. 1, 4 and 5), which is accompanied by the evolution of irreversible strain $\varepsilon_{irr}$. Thus, with increasing σ and *T*, a stress-induced MT is accompanied by the defect formation, which could be due to a low yield strength level of the martensite. The reversible strain $\varepsilon_{rev}$ is decreased by 3.5%, while the values of $\varepsilon_{irr}$ are as low as 0.3%, therefore a decrease in $\varepsilon_{rev}$ is not solely controlled by the appearing $\varepsilon_{irr}$.

The first factor, to which a decrease in the reversible strain $\varepsilon_{rev}$ could be attributed, is the change in the austenite lattice parameter prior to the MT. It is evident from the σ(ε) response (Fig. 1) that at high testing temperatures before the transformation, austenite is subjected to considerable elastic straining. This suggests that at the moment of transformation the austenite lattice (unit cell, lattice constant) is distorted. The authors of [14], using the [001]-oriented single crystals of *B*2-alloys demonstrated that in the conditions of elastic deformation prior to the beginningstress-

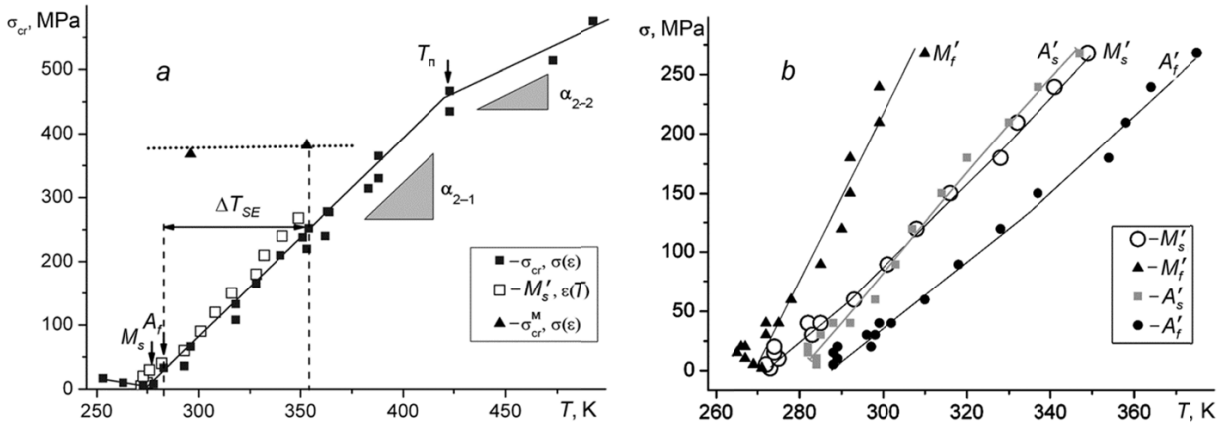


Fig. 6. Temperature dependences $\sigma_{cr}(T)$ of critical stresses of martensite formation (*a*) and the dependence of MT temperatures $M_s'$, $A_s'$, $A_f'$ and $M_f'$ during cooling/heating under loading versus applied external stress σ for the [012]-oriented $Ni_{54}Fe_{19}Ga_{27}$ single crystals in compression.

induced MT the $a_{[001]}$ lattice parameter changes by about 4.5%, while $a_{[010]}$ and $a_{[100]}$ – by about 1.5%. In this case, the difference in the austenite and martensite lattice parameters, which characterizes the value of transformation strain, becomes smaller. As the testing temperature is increasing, the elastic deformation also increases, the difference in the lattice parameters is decreased and so is the transformation strain.

Using TiNi alloys, it is shown that the variation in the reversible strain with increasing testing temperature could be attributed to the difference in the effective elastic moduli of the austenite $E_a$ and martensite $E_м$ [15]. If we associate the linear size variation of a body not only with the lattice strain but also with the elastic elongation/contraction due to differing elastic constants of the austenite $E_a$ and martensite $E_м$, then we will have an additional contribution due to the difference between $E_a$ and $E_м$ [15]

$$\varepsilon_{rev} = \varepsilon_0 + \left[\frac{1}{E_м} - \frac{1}{E_a}\right]|\sigma|, \qquad (1)$$

where $\varepsilon_0$ is the theoretical lattice strain and σ is the martensite formation stress. During compressive deformation, the effective elastic modulus of the austenite, $E_a$, in the [012]-oriented NiFeGa single crystals is lower than that of the martensite, $E_м$, so the addend in expression (1) will be negative, which might result in a decrease in the reversible strain during investigation of SE (see Fig. 1*b*). As the temperature is increased the elastic modulus of the austenite $E_a$ increases approximately twice within the temperature interval from 300 to 350 K, as evidenced by Fig. 1*b*, and the difference in the elastic moduli is significantly decreased. On the other hand, the critical stresses of martensite formation increase by a factor of 3.5. Therefore, in accordance with (1) an increase in the testing temperature and applied external stresses would cause the value of $\varepsilon_{rev}$ to decrease due to the difference in the effective elastic moduli of the austenite and martensite ($E_a < E_м$), which results in lower reversible strains during the development of SE compared to those observed for SME.

Figure 6 presents the dependence of critical stresses of martensite formation $\sigma_{cr}$ on testing temperature $T$ and the dependence of MT temperatures $M_s'$, $A_s'$, $A_f'$ and $M_f'$ during cooling/heating under loading on applied external stresses σ. For $T > M_s$, the critical stresses $\sigma_{cr}$ are those necessary for a stress-induced MT to start (Fig. 6*a*). It is evident from Fig. 6 that the $\sigma_{cr}(T)$ and $M_s'(\sigma)$ responses coincide.

The $\sigma_{cr}(T)$ dependence in the region of a stress-induced MT shows an increase following the Clapeyron–Clausius equation [15, 16] in two stages with the coefficients $\alpha_{2-1} = d\sigma_{cr}/dT =$ 3.1 MPa/K and $\alpha_{2-2}$ = 1.5 MPa/K. Stresses in stage 2–1 are those that favor the formation of the 14*M*-stress-assisted martensite. A change in the value of α occurs at $T_п$ = 423 K and is associated with the change of the MT sequence from $L2_1$–14*M*–$L1_0$ into $L2_1$–$L1_0$. A similar

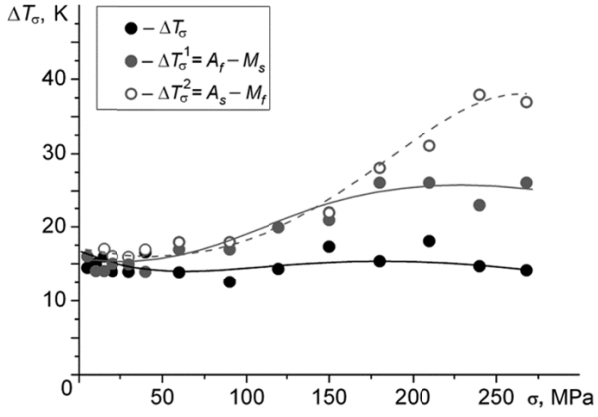


Fig. 7. Thermal hysteresis variation versus stresses ($\Delta T_\sigma(\sigma)$, $\Delta T_\sigma^1(\sigma)$ and $\Delta T_\sigma^2(\sigma)$) for the [012]-oriented NiFeGa single crystals in compression.

change in the sequence during a stress-induced MT and a stage-wise behavior of $\sigma_{cr}(T)$ were observed in NiFeGa single crystals of different orientations, for which $\varepsilon^{L1_0}_{\text{CVP+detw}} \neq \varepsilon^{14M}_{\text{CVP+detw}}$ [8, 17]. In compression, the SE curve at $T = 423$ K exhibits a yield drop typically observed during formation of the $L1_0$-martensite and during tensile loading of the [012]-oriented crystals at $T > T_T$ [17]. The values of $T_T$ depend on orientation and in the [012]-oriented single crystal are close both under compressive and tensile loading conditions [17]. In contrast to other orientations, where $\varepsilon^{L1_0}_{\text{CVP+detw}} \neq \varepsilon^{14M}_{\text{CVP+detw}}$, in the [012]-oriented single crystals in compression at $T > T_T$ an MT is accompanied by considerable plastic deformation of the martensite and not all of this strain is reversible, i.e., no SE is observed (Fig. 1).

It has been experimentally shown that SE in the [012]-oriented single crystals in compression is observed within a narrow temperature interval $\Delta T_{SE} = T_{SE2} - T_{SE1} = 353–273$ K = 80 K (Fig. 6*a*). As follows from [7, 9], it is the low values of coefficient α, high values of yield strength level of the high-temperature and martensite phases which serve a criterion of formation of the high-temperature SE. In compression, $\alpha_{2-1} = 3.1$ MPa/K, which in the [012]-oriented single crystals is by a factor of 1.5 higher and $\sigma_{cr}^M(T_{SE2}) = 382$ MPa is twice lower than those in the [001]-oriented single crystals, wherein $\alpha_2 = 2.1$ MPa/K, $\sigma_{cr}^M = 775$ MPa [9]. The interval of SE development in the [012]-oriented crystals is thus by a factor of 2.2 lower than that in the [001]-oriented crystals ($\Delta T_{SE} = 180$ K [9]).

The values of $\alpha' = 3.2$ MPa/K for the dependences $M_s'(\sigma)$, $A_s'(\sigma)$ and $A_f'(\sigma)$ are close to $\alpha_{2\text{-}1} = 3.1$ MPa/K calculated from $\sigma_{cr}(T)$. Temperature $M_f'$ increases with a large coefficient $\alpha' = 7.0$ MPa/K, that is with an increase in the externally applied stresses, loops of the $\varepsilon(T)$ curve become asymmetric, and the temperature interval $\Delta'_1$ of the forward MT extends (Fig. 4). Thus, in order to provide a complete description of the variation in the thermal hysteresis as a function of externally applied stresses, the hysteresis values were calculated as follows: 1) $\Delta T_\sigma$ – as a difference between the forward and reverse MT temperatures during cooling/heating under loading in the middle of the $\varepsilon(T)$ loop; 2) $\Delta T_\sigma^1$ and $\Delta T_\sigma^2$ – from the difference between the MT temperatures $\Delta T_\sigma^1 = |A_f' - M_s'|$ and $\Delta T_\sigma^2 = |M_f' - A_s'|$ (Fig. 7). The values of $\Delta T_\sigma$ hardly differ with increasing stresses and are found to be 15–17 K. The values of $\Delta T_\sigma^1$ and $\Delta T_\sigma^2$ increase for $\sigma = 20–150$ MPa from 15 to 22 K and then $\Delta T_\sigma^1$ changes but slightly, while $\Delta T_\sigma^2$ increases with increasing stresses up to 37 K.

Thus, an increase in the values of thermal and stress hysteresises, strain hardening coefficients and irreversible strains with increasing testing temperature confirms an increased energy dissipation during the stress-induced MT due to defect generation at low strengths of the martensite phase.

As follows from [18], relying on the thermodynamic description of a stress-induced MT, we can determine the ratio of the reversible $|\Delta G_{\text{rev}}|$ and irreversible $|\Delta G_{\text{irr}}|$ components of the non-chemical energy using an analysis of the $\varepsilon(T)$ curves. In terms of the Tong–Weimann assumption [18], neither elastic nor surface energies, contributing to $|\Delta G_{\text{rev}}|$,

are generated during nucleation of the first martensite plate on the free surface of single crystals at $T = M_s'$ (volume fraction of the martensite $\delta = 0$). Accordingly, for the last-forming plate during the reverse MT at $T = A_f'$ $|\Delta G_{rev}(0)| = 0$ as well. In the case of non-symmetrical hysteresis loops, $|\Delta G_{irr}|$ depends on the volume fraction of the martensite. Thus, the relationship between the MT temperatures derived from $\varepsilon(T)$, and $|\Delta G_{rev}|$ and $|\Delta G_{irr}|$ for $\delta = 0$ and 1 could be written in the following form [18]:

$$|\Delta G_{rev}(1)| = (M_s' - M_f')\frac{\Delta S_{ch}}{2} + (A_f' - A_s')\frac{\Delta S_{ch}}{2},$$
$$|\Delta G_{irr}(0)| = \frac{\Delta S_{ch}}{2}(A_f' - M_s'), \quad |\Delta G_{irr}(1)| = \frac{\Delta S_{ch}}{2}(A_s' - M_f'). \tag{2}$$

In expressions (2), $\Delta'_1 = M_s' - M_f'$, $\Delta'_2 = A_s' - A_f'$, $\Delta T_\sigma^1 = |A_f' - M_s'|$, $\Delta T_\sigma^2 = |M_f' - A_s'|$. Since $\Delta T_\sigma^1$ is proportional to $|\Delta G_{irr}(0)|$, and $\Delta T_\sigma^2 \sim |\Delta G_{irr}(1)|$, then, as follows from Fig. 7, for the external stresses within $\sigma = 2$–150 MPa, $|\Delta G_{irr}(0)| = |\Delta G_{irr}(1)|$, while at $\sigma > 150$ MPa, $|\Delta G_{irr}(1)| > |\Delta G_{irr}(0)|$. Thus, as the externally applied stresses increase, an increase in the values of $|\Delta G_{irr}(1)|$, compared to those of $|\Delta G_{irr}(0)|$, would suggest the presence of obstacles to phase boundary motion in the case of a forward MT during cooling/heating under loading. Similarly, during isothermal loading/unloading cycles with increasing testing temperature in the second stage of the MT, $L2_1$–$L1_0$, there is an increase in the strain hardening coefficient $\theta = d\sigma/d\varepsilon$ (see Fig. 1) and an increased stress hysteresis value due to, among other things, the difficulties of detwinning of the $L1_0$-martensite.

It has been experimentally found out that an increase in the externally applied stresses results in considerably larger intervals of the forward and reverse MTs, $\Delta'_1$ and $\Delta'_2$. Note that $\Delta'_1 > \Delta'_2$, and their difference $(\Delta'_1 - \Delta'_2)$ is also increasing with the stresses (Fig. 6). Similar non-symmetrical hysteresis loops are reported in heterophase single-crystal alloys, TiNi and NiFeGa [19, 20], which contain disperse particles. The particles undergo elastic deformation in the course of MTs and favor storage of the reversible energy. Since the values of $(\Delta'_1 + \Delta'_2)$ are proportional to that of $|\Delta G_{rev}|$, so in the case of a forward stress-induced MT during cooling/heating the stored reversible energy considerably increases.

It is the reversible $|\Delta G_{rev}|$- and irreversible $|\Delta G_{irr}|$-components of the energy, which control the relationship between the starting temperatures of the forward and reverse stress-induced transformations. From [18] and (2) follows that

$$A_s' - M_s' = \frac{1}{\Delta S_{ch}}(|\Delta G_{irr}(0)| + |\Delta G_{irr}(1)| - |\Delta G_{rev}(1)|). \tag{3}$$

The above considerations suggest that using (3) we can estimate the ratio between $|\Delta G_{rev}|$ and $|\Delta G_{irr}|$. For $\sigma < 100$ MPa $A_s' > M_s'$, hence $|\Delta G_{irr}(0)| + |\Delta G_{irr}(1)| > |\Delta G_{rev}(0)|$, thus, according to the Tong – Weimann classification, the observed transformation is a Type I MT that is accompanied by low values of the stored elastic energy. For $\sigma > 100$ MPa $M_s'$ and $A_s'$ change over, $|\Delta G_{irr}(0)| + |\Delta G_{irr}(1)| < |\Delta G_{rev}(0)|$, and the transformation is a Type II MT characterized by large stored elastic energy favoring a reverse MT. The change in the MT type could be attributed to an increased elastic modulus of the austenite $E_a$ by a factor of 2 as shown in Fig. 1*b*, implying that the elastic accommodation of the austenite and martensite at high temperatures and stresses is accompanied by higher stored elastic energies.

## SUMMARY

A systematic investigation of thermoelastic intermartensitic transformations in the [012]-oriented single crystals of $Ni_{54}Fe_{19}Ga_{27}$ (at.%) has been carried out under compressive loading and the following principles have been identified.

1. It has been experimentally demonstrated that the parameters of mechanical and functional properties of the crystals investigated under isothermal loading/unloading cycling (σ(ε))-curves) are consistent with each other, which confirms both the high quality of these single crystals and the independence of their functional properties of the testing procedure.

2. A change has been experimentally revealed in the sequence of stress-induced intermartensitic transformations from $L2_1$–14$M$–$L1_0$ at $T$ < 423 K to $L2_1$–$L1_0$ at $T$ > 423 K, which is reflected in the $\sigma_{cr}(T)$ curve as a number of stages with different values of $\alpha_{2-1} = d\sigma_{cr}/dT$ = 3.1 MPa/K and $\alpha_{2-2}$ = 1.5 MPa/K, since straining in the case of formation of the 14$M$-martensite is lower that that in the case of the $L1_0$-martensite. Within the temperature interval $T$ = 300–350 K, the stress-induced intermartensitic transformations $L2_1$–14$M$–$L1_0$ are accompanied by a number of stages in the σ(ε) response and different values of the stress hysteresis.

3. Superelasticity in the [012]-oriented single crystals of $Ni_{54}Fe_{19}Ga_{27}$ (at.%) under compressive loading is observed within a narrow temperature interval 80 K, which is determined by the high value of $\alpha_{2-1} = d\sigma_{cr}/dT$ = 3.1 MPa/K and low yield strength of the martensitic $L1_0$-phase, whose values exhibit little dependence on temperature and are equal within 368–382 MPa.

4. The maximum reversible strain of the transformation is 6.3% (the value of SME). Note that a significant contribution into the transformation strain (~30% of the total reversible strain) comes from detwinning of the $L1_0$-martensite. The reversible strain decreases with increasing testing temperature $T$ and external stresses σ, which is controlled by large elastic variations in the lattice parameter of the high-temperature phase prior to the stress-induced MT and by the differences between the austenite and martensite elastic moduli.

5. The evolution of an MT under high externally applied stresses σ > 100 MPa is accompanied by a storage of considerable reversible energy, exceeding the dissipated energy ($|\Delta G_{irr}(0)| + |\Delta G_{irr}(1)| < |\Delta G_{rev}(0)|$), a change in the shape of the ($\varepsilon(T)$ curves – the loops become asymmetric ($\Delta'_1 = M_s' - M_f' > \Delta'_2 = A_s' - A_f'$, $\Delta T_\sigma^1 = |A_f' - M_s'| < \Delta T_\sigma^2 = |M_f' - A_s'|$), and the reverse transformation starts at higher temperatures than does the forward MT ($A_s' < M_s'$) unlike the MTs at σ < 100 MPa, for which $\Delta'_1 = \Delta'_2$, $\Delta T_\sigma^1 = \Delta T_\sigma^2$ и $A_s' > M_s'$.

The work has been performed within the RF President scholarship program No. СП-6909.2013.3 and the RFBR grant No. 12-08-00573.

**REFERENCES**

1. K. Oikawa, T. Ota, T. Ohmori, *et al*., Appl. Phys. Lett., **81**, No. 27, 5201–5203 (2002).
2. Y. Sutou, N. Kamiya, T. Omori, *et al*., Appl. Phys. Lett., **84**, 1275–1277 (2004).
3. R. F. Hamilton, H. Sehitoglu, C. Efstathiou, and H. J. Maier, Acta Mater., **55**, Is. 14, 4867–4876 (2007).
4. M. M. Karpuk, D. A. Kostyk, and V. G. Shavrov, Phys. Metals Metallogr., **110**, No. 2, 138–150 (2010).
5. K. Otsuka and C. M. Wayman, Shape Memory Materials, Cambridge University Press (1998).
6. Yu. Chumlyakov, I. Kireeva, E. Panchenko, *et al*., J. Alloys and Compounds, **577**, S393–S398 (2013).
7. Yu. I. Chumlyakov, I. V. Kireeva, E. Yu. Panchenko, *et al*., Russ. Phys. J., **51**, No. 10, 1016–1036 (2008).
8. E. E. Timofeeva, E. Yu. Panchenko, Yu. I. Chumlyakov, and H. J. Maier, Russ. Phys. J., **54**, No. 12, 1427–1430 (2011).
9. E. E. Timofeeva, E. Yu. Panchenko, Yu. I. Chumlyakov, and A. I. Tagiltsev, Vestnik Tambov. Uni., **18**, Issue 4, 1617–1619 (2013).
10. C. Efstathiou, H. Sehitoglu, J. Carroll, *et al*., Acta Mater., **56**, 3791–3799 (2008).
11. Yu. I. Chumlyakov, I. V. Kireeva, I. Karaman, *et al*., Russ. Phys. J., 47, No. 9, 893–911(2004).
12. J. Dadda, H. J. Maier, I. Karaman, and Y. Chumlyakov, Int. J. Mater. Res., 101, No. 12, 1503–1513 (2010).
13. A. L. Roytburd and Ju. Slusker, Scripta Metallurg. Mater., **32**, No. 5, 761–766 (1995).
14. X. D. Ding, T. Suzuki, J. Suna, *et al*., Mater. Sci. Eng. A, **438**–440, 113–117 (2006).

15. Y. Liu and H. Yang, Mater. Sci. Eng., **A260**, 240–245 (1999).
16. E. Panchenko, Y. Chumlyakov, H. J. Maier, *et. al*., Intermetallics, **18**, 2458– 2463 (2010).
17. E. Yu. Panchenko, Yu. I. Chumlyakov, E. E. Timofeeva, *et al*., Deform. Razrush., No. 2, 22–29 (2010).
18. L. Daroczi, Z. Palanki, S. Szabo, and D. Beke, Mater. Sci. Eng., **378**, 274– 277 (2004).
19. Yu. I. Chumlyakov, I. V. Kireeva, E. Yu. Panchenko, *et al*., Russ. Phys. J., **54**, No. 8, 937–950 (2011).
20. E. Yu. Panchenko, Yu. I. Chumlyakov, I. V. Kireeva, *et al*., Phys. Metals Metallogr., **106**, No. 6, (2008).